Photoelectron Spectroscopy of Yttrium Oxide Cluster Anions: Effects of Oxygen and Metal Atom Addition

Axel Pramann, Yoshiaki Nakamura, and Atsushi Nakajima*

Department of Chemistry, Faculty of Science and Technology, Keio University, 3-14-1 Hiyoshi, Kohoku-ku, Yokohama 223-8522, Japan

Koji Kaya

Institute of Molecular Science, Myodaiji, Okazaki 444-8585, Japan

Received: February 27, 2001; In Final Form: May 28, 2001

The photoelectron spectra of small gas-phase $Y_nO_m^-$ clusters ($n = 2-10$, $m = 1-3$) are measured at photon energies of 3.49 and 4.66 eV. Cluster generation is performed with the aid of laser vaporization, whereas the kinetic energy of electrons is measured using a magnetic bottle photoelectron spectrometer. The evolution of the electronic structure of neutral yttrium oxide clusters is discussed in terms of both sequential oxygen addition to the metal cluster core and sequential metal atom increase. Electron affinities and vertical detachment energies are measured and compared to ionization potentials of the monoxide cluster series [Knickelbein, M. *J. Chem. Phys.* **1995**, *102*, 1]. A general trend in the observed photoelectron spectra is a shifting of threshold energies to higher binding energies with increasing cluster size *n*. At low electron binding energies, main spectral features are contributed from metal d-band orbitals whereas the O 2p contribution becomes apparent with increasing oxygen content due to a higher degree of hybridization of yttrium s, d, and oxygen 2p orbitals. The differences of yttrium−oxygen dissociation energies are determined and compared.

Introduction

In a couple of decades transition metal clusters in general and especially transition metal oxide clusters have become a matter of increasing interest.[1−4] This is related to the fact that bulk-phase transition metals and their oxides play an important role in materials sciences, nanotechnology, microelectronics, high-temperature chemistry, and heterogeneous catalysis.[5−7] Transition metal oxides often behave as semiconductors. The band structures of these oxides often exhibit a small overlap between the d-band of the respective metal and oxygen 2p-bands.[8]

Therefore, it is of fundamental importance to study the size dependence of electronic and geometric structures of these species, from the atom toward the bulk. Thus, isolated gas-phase clusters are well suited for the investigation of electronic and geometric structures as a function of both particle size and composition.

There exist only a few studies concerning second- or third-row transition metal and transition metal compound clusters. This is related to the fact that spectroscopic studies as well as theoretical calculations are difficult to perform due to the large amount of valence electrons and electronic states. While a broader range of experimental studies of molecular yttrium oxides has been investigated,[9−13] there are only a few studies dealing with small yttrium oxide clusters. Wu and Wang[14] have performed vibrationally resolved photodetachment studies on small yttrium oxide molecules containing one yttrium atom and up to five oxygen atoms. Knickelbein[15] has probed the ionization potentials of pure neutral yttrium clusters and their monoxides in a size range from 2 up to 31 atoms. Nevertheless, spectroscopic studies of yttrium oxide cluster anions containing more than two yttrium atoms are still lacking.

Photoelectron spectroscopy (PES) of negatively charged clusters is a tool that combines the merits of mass selection with the ability to probe the electronic structure of the neutral species in the one particle approximation. During the past decade, a large number of PES studies on transition metal chalcogenide cluster anions has been performed.[16−28]

In this article, we report on a photoelectron spectroscopic study of small yttrium oxide cluster anions $Y_nO_m^-$ ($n = 2-10$, $m = 1-3$) for the first time. Photoelectron spectra are recorded at two detachment wavelengths: 266 and 355 nm. Both electron affinities and vertical detachment energies are measured. A general motivation of this study is to screen the evolution of the electronic structure of small ($n \leq 10$) $Y_nO_m^-$ clusters with special respect to the threshold binding energy behavior. While smaller oxide clusters exhibit several spectral features, the peak shape broadens at larger cluster sizes. As a general trend, electron affinities shift to higher binding energies (BE) when both the number of yttrium atoms per cluster and the number of oxygen atoms increase. The interaction between yttrium and oxygen is discussed in terms of electronic structure and oxidation states. Furthermore, the increase of oxygen content as well as the increase of yttrium atoms per cluster provides a qualitative measure of chemisorption principles and gives insights into the nature of chemical bonding. Transition metal derived s- and d-states appear at lower BEs, while those of oxygen 2p states are located at higher BEs. The addition of oxygen clearly reveals a merging of these initially separated states. Obviously, the observed spectral features at low BE mainly result from metal s, d, and oxygen 2p valence orbital hybridization.

* Corresponding author. Fax: +81-45-566-1697. E-mail: nakajima@sepia.chem.keio.ac.jp.

10.1021/jp010749b CCC: $20.00
Published on Web 07/19/2001

Experiment

The experimental details used in this study have been reported previously,[29,30] and only a brief description will be given here.

Yttrium oxide cluster anions are generated with a pulsed laser vaporization cluster source.[31,32] The light of 532 nm photons of a Nd^{3+}:YAG laser (laser pulse energy: 25 mJ) is tightly focused onto a rotating and translating yttrium target rod (purity: 99.999%). Oxide clusters consisting of 1−4 oxygen atoms per cluster are formed due to high-temperature plasma reactions of traces of oxygen present on the target surface. Under these experimental conditions, no additional mixing of the helium carrier gas (5 atm) with oxygen is needed. After formation in a 3-mm diameter channel, the clusters undergo a supersonic beam expansion resulting in the production of a vibrationally cooled molecular beam.

Subsequently, the cluster anions are detected and mass-analyzed 2.2 m downstream with an in-line time-of-flight mass spectrometer. The mass resolution, $m/\Delta m$, is about 150, which is sufficient to separate the oxide clusters in the investigated mass region. Additionally, the in-line design guarantees a high ion density in the center region of the following photodetachment experiment.

After deceleration, the mass-selected cluster anions are investigated with a magnetic-bottle-type photoelectron spectrometer,[33−35] which is located perpendicular to the molecular beam axis. When the cluster anions arrive at the turn-around point of the deceleration region,[36] photoelectron spectra are recorded using the third (355 nm: 3.49 eV) or the fourth (266 nm: 4.66 eV) harmonics of a second Q-switched Nd^{3+}:YAG laser. The applied detachment laser power is 10−20 mJ/cm^2 for 355 nm, and 1−3 mJ/cm^2 for 266 nm. After carefully scanning the laser power, no change in the shape of the photoelectron spectra is observed. Thus, we can exclude photofragmentation processes. Lower photon energies yield higher resolved spectra, while higher photon energies cover a broader spectral range. The kinetic energy of the photoelectrons is measured and converted to the electron binding energy, given by the difference of the respective photon energy and kinetic energy. The photoelectron spectrometer is calibrated using the strong transitions $^1S_0 \rightarrow {}^2S_{1/2}$ and $^1S_0 \rightarrow {}^2D_{5/2}$ of the gold atom.[37] The energy resolution (fwhm) of the photoelectron spectrometer is better than 50 meV at 1 eV electron kinetic energy and 4.66 eV photon energy. Each photoelectron spectrum is recorded and accumulated for 10000−25000 shots at 10 Hz repetition rate.

Results and Discussion

A. Mass Spectra of $Y_nO_m^-$. Figure 1 shows a typical time-of-flight mass spectrum of $Y_nO_m^-$ clusters. The oxides are formed due to plasma reactions between oxide layers on the yttrium rod surface and yttrium using a nonseeded pure helium carrier gas. During the experiments, no pure Y_n^- clusters have been observed at all. This phenomenon can occur when studying highly reactive open d-shell anionic species,[38] and indicates lower electron affinities of the pure neutral metal clusters compared to their oxides.

The mass spectrum is dominated by yttrium oxide cluster anions $Y_nO_m^-$ in the size range $n = 2-10$. At each number of yttrium atoms per cluster a multiplet pattern of oxide peaks occurs, starting from the respective monoxide up to $m = 4$, the latter in lower abundance. The appearance of both even- and odd-numbered oxide clusters is also a first indication of both molecular and dissociative oxygen chemisorption. $Y_3O_2^-$ is always the most abundant and stable oxide cluster. In this oxide, yttrium has a formal oxidation state of +1, assuming an oxidation state of −2 for the oxygen atom. From $n \geq 4$, the respective monoxide exhibits the highest abundance and the question arises whether the accompanying oxides ($m \geq 2$) are successively added. Due to low intensities of higher oxides ($m \geq 3$), mainly the monoxides and dioxides are probed by photodetachment photoelectron spectroscopy.

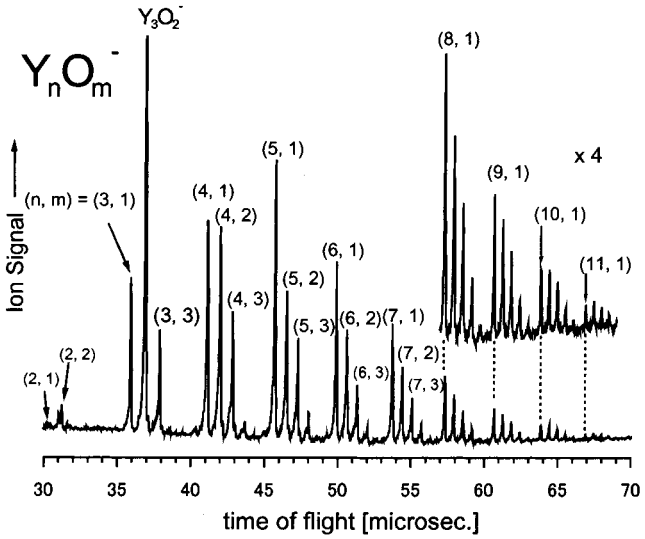

Figure 1. Typical time-of-flight mass spectrum of $Y_nO_m^-$ clusters. Oxide cluster anions are formed by plasma reactions of oxygen traces on the target surface and yttrium using a pure helium carrier gas. $Y_3O_2^-$ is always the most abundant species. Note that under the current experimental conditions no pure Y_n^- clusters are formed.

TABLE 1: Electron Affinities (EA) and Vertical Detachment Energies (VDE) of Y_nO_m Clusters[a]

cluster size (n, m)	EA [eV]	VDE [eV]
2, 2	1.29(14)	1.45(09)
3, 1	1.10(19)	1.33(08)
3, 2	1.44(23)	1.71(11)
3, 3	1.29(30)	1.68(16)
4, 1	1.05(12)	1.19(04)
4, 2	1.19(21)	1.45(09)
4, 3	1.38(29)	1.75(15)
5, 1	1.17(23)	1.47(11)
5, 2	1.14(18)	1.35(07)
5, 3	1.24(33)	1.62(18)
6, 1	1.23(20)	1.47(08)
6, 2	1.17(21)	1.43(09)
7, 1	1.21(30)	1.61(15)
7, 2	1.24(31)	1.65(11)
8, 1	1.34(28)	1.72(15)
8, 2	1.34(30)	1.73(16)
9, 1	1.32(22)	1.58(10)
10, 1	1.48(23)	1.82(11)

[a] Numbers in parentheses indicate uncertainties of the last digits; 1.38(29) is a shortcut for 1.38 ± 0.29 eV.

Under the applied mild oxidation conditions, no closed shell oxides such as YO_2^-, $Y_3O_5^-$, $Y_5O_8^-$, or $Y_7O_{11}^-$ are observed, even if these species should be the most thermodynamic stable oxides when assuming an oxidation state of −2 for the oxygen atom and +3 for the yttrium atom, which has a [Kr]4d5s^2 valence electron configuration.

B. Photoelectron Spectroscopy of Small $Y_nO_m^-$ Clusters. Photoelectron spectra are measured using 3.49 and/or 4.66 eV photon energies. In the case of the one particle approximation for the process $Y_nO_m + e^- \leftarrow Y_nO_m^-$, the spectra show the electronic transitions from the ground state of the anionic precursor to ground or excited states of the respective neutral species in the geometry of the anion. Therefore, broader

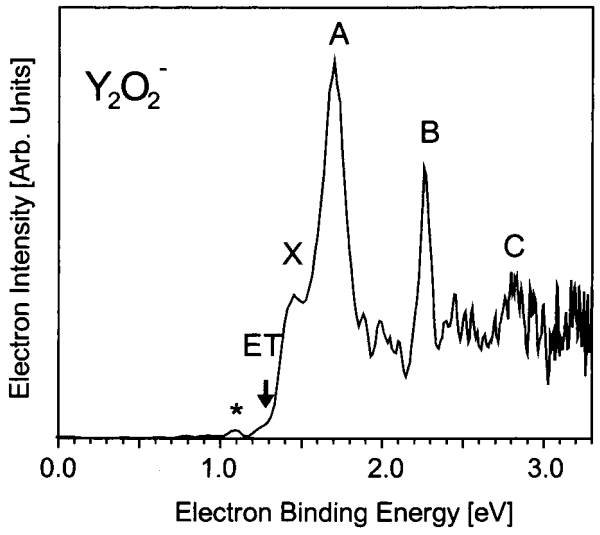

Figure 2. Photoelectron spectrum of $Y_2O_2^-$ taken at 355 nm (3.49 eV photon energy). The asterisk at 1.1 eV binding energy is tentatively attributed to an isomer. The downward arrow indicates the threshold binding energy (EA).

photoelectron signals indicate a geometry change between the anionic and neutral cluster.

Threshold binding energies (ET) are determined as upper limits of adiabatic electron affinities (EA) from the onset of each photoelectron spectrum at 10% of the first peak maximum. In the following, ET are handled as electron affinities (EA). The more sharp the onset of the first PES peak, the better the agreement with the adiabatic electron affinity, which can be determined only if there exists a proper overlap between the Franck−Condon factors of the neutral and anionic ground states. Additionally, vertical detachment energies (VDE) are determined from the photoelectron peak maxima. Both EA and VDE values are listed in Table 1.

B.1. Photoelectron Spectrum of $Y_2O_2^-$. Figure 2 shows the photoelectron spectrum of $Y_2O_2^-$ taken at 3.49 eV photon energy. The $Y_2O_2^-$ cluster is the smallest we are able to study, since its mass spectral abundance is always very low. The electron affinity of Y_2O_2 is determined to 1.29(14) eV and marked by a downward arrow. The spectrum is dominated by two sharp peaks, labeled as the A and the B states, respectively. On the rising binding energy side of the A peak, a smaller clear resolved peak X on the shoulder of A is observed. The X-labeled peak corresponds to the transition from the ground electronic state of the anion, $Y_2O_2^-$, to the ground electronic state of the neutral cluster. This transition occurs at the first vertical detachment energy at 1.45(09) eV. The origin of the X peak is not a hot band transition nor due to an isomer since after varying the source conditions the X signal is always observed. Therefore, we can assign it to a true first transition from the anion to the neutral. Another reason for the lower intensity of the X-labeled peak is a relatively low photodetachment cross section for this ground state transition. Even though there is a considerable overlap between this ground state transition peak with the strong signal labeled A, the X signal indicates a similar rigid structure of both the anion and the neutral due to a sharp onset. We tentatively assign the peaks A, B, C at 1.70, 2.26, and 2.78 eV as the electronic transitions from the ground state of the anion to the first, second, and third excited state of the neutral cluster. Due to a poor signal-to-noise ratio at the higher BE scale, the higher states cannot be determined accurately. The first VDE

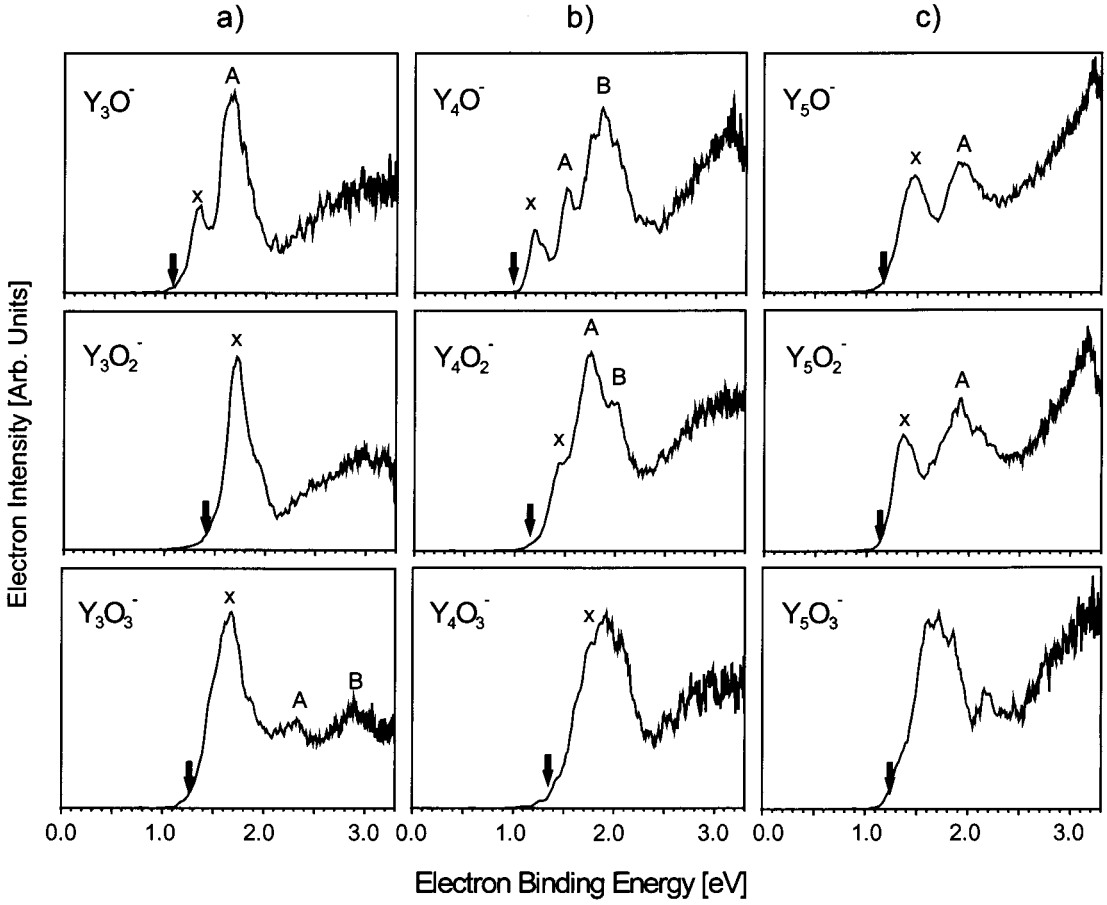

Figure 3. Photoelectron spectra of Y_3O^-, $Y_3O_2^-$, and $Y_3O_3^-$ (a); Y_4O^-, $Y_4O_2^-$, and $Y_4O_3^-$ (b); Y_5O^-, $Y_5O_2^-$, and $Y_5O_3^-$ (c) taken at 355 nm.

is separated by only 250 meV from the ground-state transition, which contributes to a relatively small term value of the A state. Generally, PE spectra of transition metal clusters and transition metal compound clusters such as oxides reveal a large number of low-lying electronic states. Due to this fact and limited by our experimental resolution we are not able to detect and assign many different electronic states. But our main intention is not to determine every single state but to show the general size-dependent evolution of the electronic structure of the clusters using a high detection efficiency. The spectral features are mainly contributed by yttrium 4d and 5s molecular orbitals, which are located at the lower binding energy side. This can be deduced from theoretical calculations of electronic structures of transition metal oxides in general and also from those of Y−O.[39] As can clearly be seen for larger clusters sizes ($n \geq 4$) in the next subsection the yttrium 4d, 5s, and oxygen 2p orbitals merge with increasing number of oxygen atoms per cluster which demonstrates the hybridization effect. The chemical bonding between Y and O atoms mainly results from the interaction between the 4d and 5s orbitals of yttrium and 2p orbitals of oxygen. Therefore, the electron transfer in yttrium−oxygen bonds is directed from the yttrium d-orbitals to the oxygen 2p orbitals. The geometric structures of both $Y_2O_2^-$ and Y_2O_2 are most likely rhombuses of D_{2h} geometry with alternating Y and O atoms as in the case of sulfur transition metal compounds such as $Mn_2S_2^-$[25] and $Fe_2S_2^-$[26]. This assumption is quite reasonable, since oxygen and sulfur have both the same outer valence electron configuration, although more reliable ab initio structural calculations are necessary.

The small bump labeled with an asterisk at the low binding energy side is assumed to have its origin in an isomer with low electron affinity. Its appearance depends on the cluster source conditions. Wang and co-workers have observed similar isomers in the case of ScO_2 and YO_2 molecules.[14] In this case, the structure of the $Y_2O_2^-$ isomer is most probably a neutral Y_2 unit with a side-bonded peroxide (O_2^{2-}) anion.

B.2. Photoelectron Spectra of $Y_3O_m^-$, $Y_4O_m^-$, and $Y_5O_m^-$ ($m = 1-3$). Figure 3a−c shows the photoelectron spectra of $Y_3O_m^-$, $Y_4O_m^-$, and $Y_5O_m^-$ ($m = 1-3$), respectively, taken at 355 nm. Electron affinities and vertical detachment energies are listed in Table 1 and are shown in Figure 4. In the $Y_3O_m^-$ series (Figure 3a), all spectra are dominated by a strong sharp peak around 1.5 eV binding energy, similar to the A-labeled peak of the $Y_2O_2^-$ spectrum in Figure 2. Threshold binding energies are indicated by downward arrows and show no regular size dependence. This is an often observed criterion of quantum size effects of very small clusters. Whereas the PE spectra of $Y_3O_2^-$ and $Y_3O_3^-$ are very similar, the spectrum of Y_3O^- exhibits also a small peak X at the low binding energy side, similar to $Y_2O_2^-$. The geometric structure of Y_3O^- is most probably a planar C_{2v} structure with a doubly bridging oxygen atom very similar as in the case of V_3O^-, Nb_3O^-, and Ta_3O^- which are reported in a recent paper of Leopold and co-workers using high-resolution negative ion PES.[23] Even though accurate structural ab initio calculations are not yet available for the $Y_nO_m^-$ clusters, the simple comparison of the spectral shapes gives a first indication of possible geometric structures. The PE spectra reported in ref 23 show all very sharp intense signals of the ground-state transitions around 1.2 to 1.6 eV as in the case of Y_3O^-. Since the extra electron of the anion of the early transition metals occupies a nonbonding orbital, it is reasonable to predict a similar geometric structure for Y_3O^-. Y_3O_2 reveals a higher electron affinity than Y_3O and Y_3O_3. Also the peak shape is sharper than in the case of neighboring oxide clusters. This

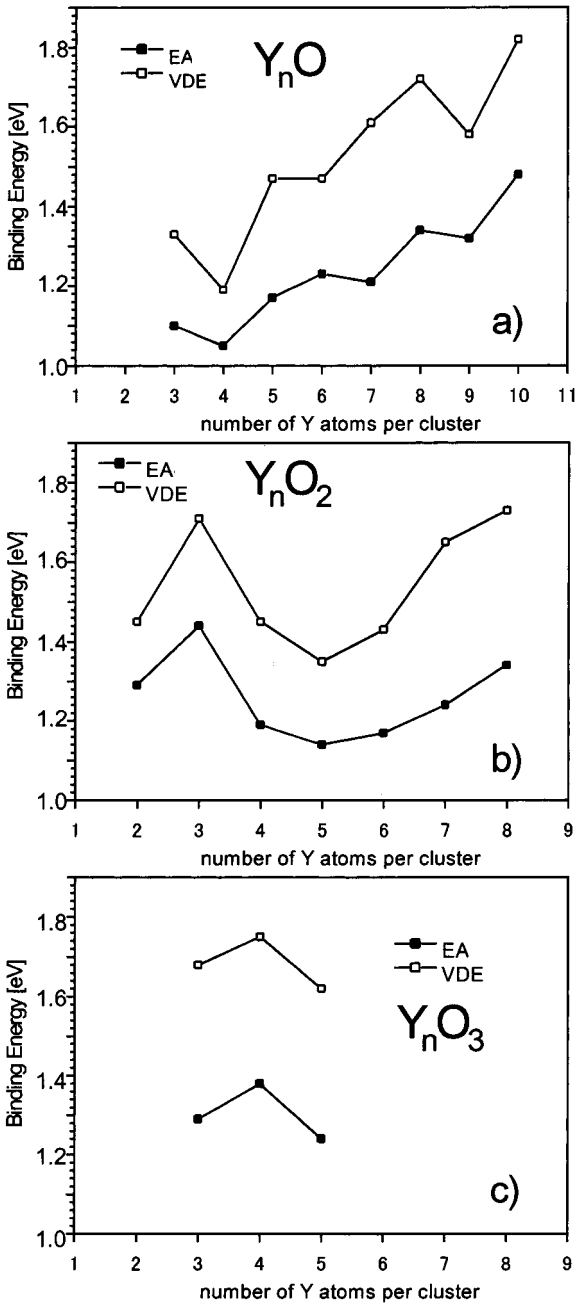

Figure 4. Electron affinities (EA) and vertical detachment energies (VDE) of Y_nO, Y_nO_2, and Y_nO_3 clusters. For more clarity, error bars are not displayed (see Table 1).

corresponds very well to the high mass spectrometric abundance of this oxide, indicating a high stability due to both geometric as well as electronic effects. Additionally, for this cluster the geometry change between the anion and the neutral species is small. Generally, a more simple spectral shape with increasing number of oxygen atoms is observed. The several spectral features at the low-binding-energy side appear when only one oxygen atom is attached onto the yttrium cluster surface. Therefore, the signals X and A are mainly contributed by yttrium metal d and s valence orbitals. After the addition of more oxygen atoms to the cluster core, the spectrum is also influenced by oxygen 2p orbital contributions, thus a hybridization effect between yttrium s and d and oxygen 2p orbitals will increase with increasing number of oxygen atoms. After that intense peak, a second less-resolved broad band appears with increasing intensity toward higher BE, which might be contributed by

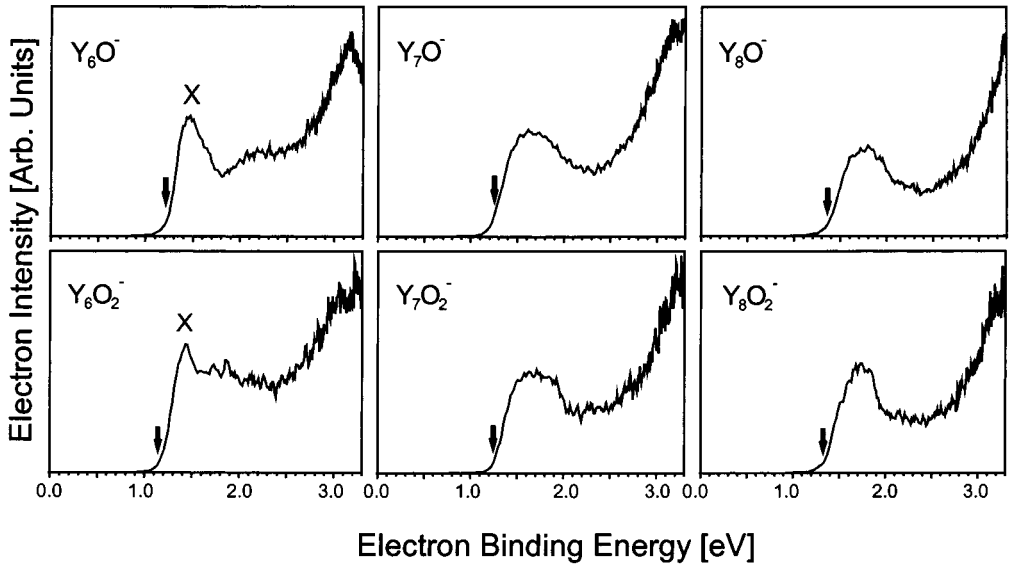

Figure 5. Photoelectron spectra of Y_6O^-, $Y_6O_2^-$, Y_7O^-, $Y_7O_2^-$, Y_8O^-, and $Y_8O_2^-$, taken at 355 nm.

oxygen 2p orbitals. The similarity of the spectral shapes in Figure 3 suggests an initial yttrium cluster core with additional oxygen atoms attached onto the metal cluster surface.

The next series containing four yttrium atoms per cluster (see Figure 3b) is also dominated by one intense, but broader signal, which is shifted to higher binding energies compared to the $Y_3O_m^-$ series. The low BE monoxide signal is split into several clear distinguishable peaks, which merge with increasing number of oxygen atoms: again a clear indication of oxygen 2p and metal 4d 5s molecular orbital mixing. Y_4O exhibits an electron affinity of only 1.05 eV, which is the lowest of the investigated oxides. With increasing number of oxygen atoms, the EA as well as the VDE increases, which is an often observed behavior in metal oxide cluster series. Again, the multiplet of low BE peaks labeled X, A, B in the Y_4O^- spectrum is contributed to the high influence of the metal valence molecular orbitals.

The yttrium pentamer oxide cluster series (Figure 3c) shows more different spectral features. Here, the spectra of the monoxide, Y_5O^- and the dioxide $Y_5O_2^-$ both exhibit a double peak with a gap of around 0.3 eV. In the $Y_5O_3^-$ spectrum these two peaks merge into a broad band. With increasing oxygen content, this merging is due to a more effective mixing of oxygen and metal valence molecular orbitals. The origin of the double peak in the case of the monomer and dimer is most probably due to yttrium s and p orbitals. Since the metal atom content is increased, one would expect a higher influence of the yttrium cluster core and, therefore, lower intense signals on the high BE side. But at a cluster core size of five yttrium atoms, the geometry can change from two to three dimensions. Actually, in a three-dimensional configuration the additional oxygen atoms have a higher possibility of bonding interactions with yttrium, which results in a higher degree of hybridization as is clearly seen in the merging of the X and A peak, when adding one oxygen atom after the other. Therefore, the spectrum of $Y_5O_3^-$ is dominated by a broad first unresolved peak.

B.3. Photoelectron Spectra of $Y_6O_m^-$, $Y_7O_m^-$, $Y_8O_m^-$ (m = 1−2). The photoelectron spectra of the series of $Y_6O_m^-$, $Y_7O_m^-$, and $Y_8O_m^-$ clusters with $m = 1-2$ (all taken at 3.49 eV photon energy) are shown in Figure 5. For the $n = 6$, 7, and 8 series only the monoxides and dioxides are investigated due to a low mass abundance of larger oxides. Generally, with increasing number of yttrium atoms per cluster the spectral features get broader and shift slightly to higher binding energies. Additionally, both the monoxide and the dioxide spectra are very similar for $n = 6$ to 8. For Y_6O^- and $Y_6O_2^-$ a relative sharp peak (X) occurs which merges in the case of the dioxide with oxygen valence molecular orbitals. Therefore, in the 1.5 to 2.5 eV BE region the gap-like feature diminishes. The PE spectra of Y_7O, $Y_7O_2^-$, Y_8O^-, and $Y_8O_2^-$ look quite similar each with a broad intense signal around 1.7 eV binding energy. The similar electronic structure in this size range is a first indication of the beginning of the evolution of bulklike behavior. The electronic structure of these clusters is dominated by the influence of the pure metal cluster core, because the addition of oxygen shows no remarkable change in the spectral features. Therefore, the spectral information which we can obtain in this size range is rather scarce. At the high BE side of each spectrum a very intense band above 3 eV BE can be attributed to the oxygen 2p molecular orbitals.

B.4. Photoelectron Spectra of Y_9O^- and $Y_{10}O^-$. The PE spectra of the largest investigated species Y_9O^- and $Y_{10}O^-$ are taken at 4.66 eV photon energy (266 nm). The spectra show very similar features compared to those of $n = 7$ and 8 with one intense broad peak at lower BE and an intense, rising signal at the high-binding-energy side around 4 eV. The origin of the first broad signal around 1.6 and 1.8 eV is attributed to the d and s molecular orbitals of the yttrium cluster core. As a general behavior, electron affinities and vertical detachment energies shift to higher values in the case of the probed monoxides.

B.5. The Effect of Metal Atom Addition: Y_nO^- and $Y_nO_2^-$. Another interesting point is the investigation of the influence of successive metal atom addition in the viewpoint of the electronic structure. In Figure 6 PE spectra are shown for the monoxide series Y_nO^- (starting with $n = 3$ up to $n = 9$) and the dioxide series $Y_nO_2^-$ ($n = 2-8$) taken at 3.49 eV photon energy. A vertical dotted line indicates a BE of 1.0 eV. While for the monoxides a clear shift of the threshold binding energies to higher values (EA(Y_3O) = 1.10 eV; EA(Y_9O) = 1.32 eV) can be observed, there is no regular behavior in the case of the dioxides, even if their threshold energies also shift to higher BE for larger clusters. This is a simple effect of the addition of a second oxygen atom to the monoxide, which leads to a higher degree of hybridization of yttrium s and d and oxygen 2p orbitals. Second, the spectral features become more simple and broader with increasing cluster size *n*. This behavior is already discussed and a result of a more bulklike electronic structure,

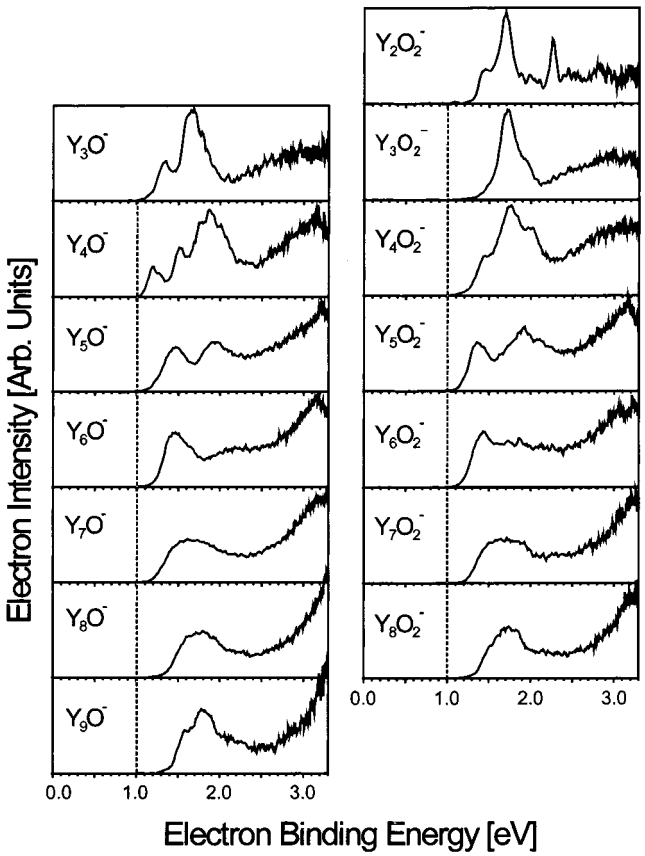

Figure 6. Photoelectron spectra of yttrium cluster monoxide anions Y_nO^- ($n = 3-9$) and $Y_nO_2^-$ ($n = 2-8$) taken at 355 nm. The vertical dashed line indicates the BE of 1 eV.

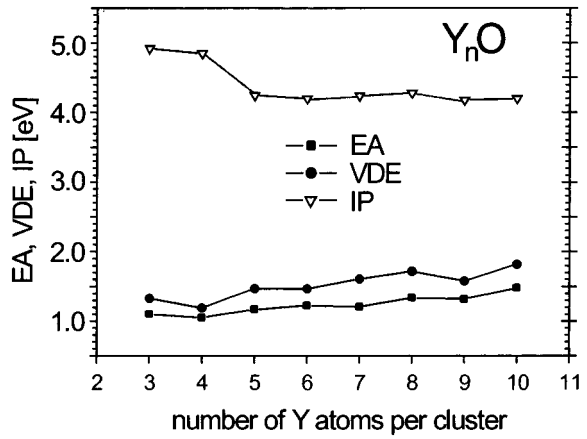

Figure 7. Electron affinities (EA), vertical detachment energies (VDE), and ionization potentials (IP) of yttrium monoxide clusters Y_nO ($n = 3-10$). IP values are taken from ref 15.

dominated by the yttrium cluster core. The most obvious differences in electronic stuctures between monoxides and dioxides are occurring at $n \leq 6$ due to the fact that the number of low-lying excited electronic states is strongly increasing.

B.6. Comparison of EA, VDE, and IP of Small Y_nO Clusters. The knowledge of the size-dependence of the electronic and geometric structures of clusters can be useful for a correlation or anticorrelation with their chemical reactivity. This method has been applied to few transition metal cluster systems,[40−42] which are most important as possible active centers in heterogeneous catalysis. Figure 7 shows a plot of electron affinities (EA), vertical detachment energies (VDE), and ionization potentials (IP, measured by Knickelbein[15]) of small Y_nO clusters ($n = 3-10$) as a function of cluster size n. For a better comparison, EA, VDE, and IP values are plotted on the same energy scale. The course of EA and VDE curves is similar. Therefore, it is sufficient to compare the EA and IP values. Very small clusters of transition metals usually have low electron affinities and comparable high ionization potentials. With increasing cluster size, both values merge into the bulk work function. For the Y_nO clusters, a similar behavior is expected and can be observed in Figure 7. The EA values increase from 1.10 for Y_3O to 1.48 eV for $Y_{10}O$, whereas the IPs decrease in the same size region from 4.92 to 4.20 eV. At $Y_{10}O$, the difference IP − EA is almost reduced to at least 2.7 eV. Both curves show no smooth or regular course, and also even/odd alternations, which are well-known in free-electron metal clusters such as alkali, coinage metal, or aluminum clusters, cannot be observed. As reported by Knickelbein,[15] at $n = 4$ a sudden change in the IP curvature is observed. This is also obvious for the EA values. From $n = 3$ to $n = 4$ the EA decreases and starts to increase at a cluster size for $n \geq 4$. The lack of a regular size pattern in the behavior of both EA and IP seems to have its origin the elimination of more localized 4d electrons during photodetachment, but additionally, at $n = 5$ again a geometrical factor—the transition from two to three dimensions must be considered.

B.7. Relative Yttrium−Oxygen Dissociation Energies. Using simple thermodynamic cycles, it is possible to determine dissociation energies, or at least differences of dissociation energies, for the chemisorption processes of oxygen on a cluster surface. As discussed in the previous sections, some clusters form favorable isomers such as the alternating ring structure of $Y_2O_2^-$: $-Y-O-Y-O-^-$. Therefore, the energy barrier for an oxygen intercalation into a cluster surface can be estimated by the dissociation energy which is needed for the loss of a single oxygen anion. We have calculated relative dissociation energies for the processes $Y_nO_m^- \rightarrow Y_nO_{m-1} + O^-$ for the monoxide, dioxide, and trioxide clusters using the following relations:

$$Y_nO^- \rightarrow Y_n + O^- \quad (1)$$

$$D_0(Y_n - O^-) - D_0(Y_n - O) = EA(Y_nO) - EA(O) \quad (2)$$

$$Y_nO_2^- \rightarrow Y_nO + O^- \quad (3)$$

$$D_0(Y_nO - O^-) - D_0(Y_nO - O) = EA(Y_nO_2) - EA(O) \quad (4)$$

$$Y_nO_3^- \rightarrow Y_nO_2 + O^- \quad (5)$$

$$D_0(Y_nO_2 - O^-) - D_0(Y_nO_2 - O) = EA(Y_nO_3) - EA(O) \quad (6)$$

Since the electron affinity of atomic oxygen (EA = 1.461 eV[43]) is accurately known, we are able to calculate the left side of eqs 2, 4, and 6, which we will call relative dissociation energies (ΔD_0). The ΔD_0 values are listed in the right column of Table 2. For the monoxide, dioxide, and trioxide clusters the amount of ΔD_0 is in the small range of 100 to 400 meV, which indicates a similar geometric framework of both neutrals and anionic clusters when dissociating by the loss of a single oxygen atom. The similar geometric structure of both anions and neutrals of the same composition is also qualitatively expected when regarding the sharp onset of the photoelectron threshold energies.

TABLE 2: Differences of the Dissociation Energies of the Y_nO^-, $Y_nO_2^-$, and $Y_nO_3^-$ Cluster Series for the Processes $Y_n - O_m^- \rightarrow Y_nO_{m-1} + O^-$

cluster size n (Y_nO^-)	$D_0(Y_n - O^-) - D_0(Y_n - O)$ [eV]
3	−0.36(6)
4	−0.41(4)
5	−0.29(5)
6	−0.23(3)
7	−0.25(6)
8	−0.12(2)
9	−0.14(2)

cluster size n ($Y_nO_2^-$)	$D_0(Y_nO - O^-) - D_0(Y_nO - O)$ [eV]
2	−0.17(2)
3	−0.02(0)
4	−0.08(1)
5	−0.32(5)
6	−0.29(5)
7	−0.22(5)
8	−0.12(2)

cluster size n ($Y_nO_3^-$)	$D_0(Y_nO_2 - O^-) - D_0(Y_nO_2 - O)$ [eV]
3	−0.17(3)
4	−0.08(1)
5	−0.22(5)

A size dependence of these values is not observed. This indicates the same oxidation mechanism for both small and larger clusters.

Conclusions

Mass selected $Y_nO_m^-$ cluster anions with $n = 2-10$ are investigated by photoelectron spectroscopy for the first time using 355 and 266 nm for the detachment wavelengths. Electron affinities and vertical detachment energies are measured. The very intense mass spectrometric abundance of $Y_3O_2^-$ can be explained by a high electron affinity (1.44 eV) of the neutral cluster among this series. The PE spectrum of $Y_2O_2^-$ shows sharp transitions to at least the first two excited states of the neutral cluster. For the monoxide series EA values are compared to IP values, and both show a nonmonotonic but clear progression with cluster size toward bulk work function. Generally, threshold energies shift to higher binding energies with increasing cluster size n. At low BE, the electronic structures are dominated by the influence of yttrium s and d valence molecular orbitals which merge with oxygen 2p orbitals with increasing number of oxygen atoms m. Therefore, clusters with lower oxygen content and smaller n reveal more sharp spectral features. Dissociation energy differences of the yttrium−oxygen bond indicate similar geometric structures of neutral and anionic clusters. To screen the evolution toward bulk-phase electronic behavior, it will be helpful to probe larger cluster sizes. Additionally, we hope that this study will motivate more indispensable theoretical structural calculations.

Acknowledgment. This work is supported by a program entitled "Research for the Future (RFTF)" of Japan Society for the Promotion of Science (98P01203) and by a Grant-in-Aid for Scientific Research (C) (No. 11640512) from the Ministry of Education, Science, Sports and Culture. A.P. gratefully acknowledges a postdoctoral fellowship from the Japan Society for the Promotion of Science (JSPS).

References and Notes

(1) See, for example: *Advances in Metal and Semiconductor Clusters*; Duncan, M. A., Ed.; JAI Press: 1993−1998; Vols. 1−4.

(2) Morse, M. D. *Chem. Rev.* **1986**, *86*, 1049.

(3) Castleman, A. W., Jr.; Bowen, K. H., Jr. *J. Phys. Chem.* **1996**, *100*, 12911.

(4) Jena, P.; Rao, B. K.; Khanna, S. N. *Physics and chemistry of small clusters*; Plenum: New York, 1987.

(5) Henrich, V. E.; Cox, P. A. *The Surface Science of Metal Oxides*; Cambridge University Press: New York, 1994.

(6) Rao, C. N. R.; *Annu. Rev. Phys. Chem.* **1989**, *40*, 291.

(7) *Transition metal oxides: surface chemistry and catalysis*. In *Studies in Surface Science and Catalysis*; Kung, H. H., Ed.; Elsevier: New York, 1989; Vol. 45.

(8) Cox, P. A. *The Electronic Structure and Chemistry of Solids*; Oxford University Press: New York, 1987.

(9) Huber, K. P.; Herzberg, G. *Molecular Spectra and Molecular Structure IV: Constants of Diatomic Molecules*; Van Nostrand Reinhold: New York, 1979.

(10) Clemmer, D. E.; Dalleska, N. F.; Armentrout, P. B. *Chem. Phys. Lett.* **1992**, *190*, 259.

(11) Sievers, M. R.; Chen, Y.-M.; Armentrout, P. B. *J. Chem. Phys.* **1996**, *105*, 6322.

(12) Sievers, M. R.; Armentrout, P. B. *Inorg. Chem.* **1999**, *38*, 397.

(13) Linton, C.; Simard, B.; Loock, H. P.; Wallin, S.; Rothschopf, G. K.; Gunion, R. F.; Morse, M. D.; Armentrout, P. B. *J. Chem. Phys.* **1999**, *111*, 5017.

(14) Wu, H.; Wang, L.-S. *J. Phys. Chem.* **1998**, *102*, 9129.

(15) Knickelbein, M. *J. Chem. Phys.* **1995**, *102*, 1.

(16) Wenthold, P. G.; Jonas, K.-L.; Lineberger, W. C. *J. Chem. Phys.* **1997**, *106*, 9961.

(17) Wu, H.; Wang, L.-S. *J. Chem. Phys.* **1997**, *107*, 16.

(18) Wu, H.; Wang, L.-S. *J. Chem. Phys.* **1997**, *107*, 8221.

(19) Wu, H.; Wang, L.-S. *J. Chem. Phys.* **1998**, *108*, 5310.

(20) Wu, H.; Desai, S. R.; Wang, L.-S. *J. Am. Chem. Soc.* **1996**, *118*, 5296.

(21) Moravec, V. D.; Jarrold, C. C. *J. Chem. Phys.* **1998**, *108*, 1804.

(22) Klopcic, S. A.; Moravec, V. D.; Jarrold, C. C. *J. Chem. Phys.* **1999**, *110*, 10216.

(23) Green, S. M. E.; Alex, S.; Fleischer, N. L.; Millam, E. L.; Marcy, T. P.; Leopold, D. G. *J. Chem. Phys.* **2001**, *114*, 2653.

(24) Klingeler, R.; Lüttgens, G.; Pontius, N.; Rochow, R.; Bechthold, P. S.; Neeb, M.; Eberhardt, W. *Eur. Phys. J. D* **1999**, *9*, 263.

(25) Zhang, N.; Kawamata, H.; Nakajima, A.; Kaya, K. *J. Chem. Phys.* **1996**, *104*, 36.

(26) Zhang, N.; Hayase, T.; Kawamata, H.; Nakao, K.; Nakajima, A.; Kaya, K. *J. Chem. Phys.* **1996**, *104*, 3413.

(27) Nakajima, A.; Kawamata, H.; Hayase, T.; Negishi, Y.; Kaya, K. *Z. Phys. D* **1997**, *40*, 17.

(28) Pramann, A.; Rademann, K. To be published.

(29) Nakajima, A.; Taguwa, T.; Hoshino, K.; Sugioka, T.; Naganuma, T.; Ono, F.; Watanabe, K.; Nakao, K.; Konishi, Y.; Kishi, R.; Kaya, K. *Chem. Phys. Lett.* **1993**, *214*, 22.

(30) Negishi, Y.; Yasuike, T.; Hayakawa, F.; Kizawa, M.; Yabushita, S.; Nakajima, A.; Kaya, K. *J. Chem. Phys.* **2000**, *113*, 1725.

(31) Dietz, T. G.; Duncan, M. A.; Powers, D. E.; Smalley, R. E. *J. Chem. Phys.* **1981**, *74*, 6511.

(32) Bondybey, V. E.; English, J. H. *J. Chem. Phys.* **1981**, *74*, 6978.

(33) Kruit, P.; Read, F. H. *J. Phys. E* **1983**, *16*, 313.

(34) Cheshnovsky, O.; Yang, S. H.; Pettiette, C. L.; Craycraft, M. J.; Smalley, R. E. *Rev. Sci. Instrum.* **1987**, *58*, 2131.

(35) Ganteför, G.; Meiwes-Broer, K.-H.; Lutz, H. O. *Phys. Rev. A* **1988**, *37*, 2716.

(36) Handschuh, H.; Ganteför, G.; Eberhardt, W. *Rev. Sci. Instrum.* **1995**, *66*, 3838.

(37) Hotop, H.; Lineberger, W. C. *J. Phys. Chem. Ref. Data* **1975**, *4*, 539.

(38) Yang, S.; Knickelbein, M. B. *Z. Phys. D* **1994**, *31*, 199.

(39) Strauss, M.; Stevens, W. J. *J. Chem. Phys.* **1985**, *82*, 5584, and references therein.

(40) Whetten, R. L.; Cox, D. M.; Trevor, D. J.; Kaldor, A. *Phys. Rev. Lett.* **1985**, *54*, 1494.

(41) Conceicao, J.; Laaksonen, R. T.; Wang, L.-S.; Guo, T.; Nordlander, P.; Smalley, R. E. *Phys. Rev. B* **1995**, *51*, 4668.

(42) Kietzmann, H.; Morenzien, J.; Bechthold, P. S.; Ganteför, G.; Eberhardt, W. *J. Chem. Phys.* **1998**, *109*, 2275.

(43) Hotop, H.; Lineberger, W. C. *J. Phys. Chem. Ref. Data* **1985**, *14*, 731.